

Magnetohydrodynamic simulations of A-type stars: Long-term evolution of core dynamo cycles.

Juan Pablo Hidalgo

Collaborators : Dominik Schleicher
: Petri Käpylä
Felipe Navarrete
Carolina Ortiz-Rodríguez

Universidad de Concepción, Chile.



Stellar structure

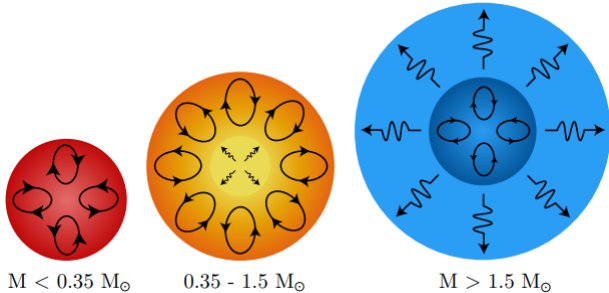


Figure: Diagram of convective and radiative zones for different ranges of stellar masses. Stars with $M \lesssim 0.3M_{\odot}$ are fully convective, intermediate mass stars have a radiative core and a convective envelope. Finally, stars with $M \gtrsim 1.5M_{\odot}$ have convective cores and radiative envelopes.

Astrophysical Dynamos

We refer to a *dynamo* as any process of amplification and maintenance of magnetic fields inside a plasma.

$$\frac{\partial \mathbf{B}}{\partial t} = \nabla \times (\mathbf{U} \times \mathbf{B}) + \eta \nabla^2 \mathbf{B}$$

These processes are most likely to occur inside the convection zones (see [Brandenburg & Subramanian 2005](#)), where $\mathbf{U} \neq 0$.

Early-type stars observed magnetism

Ap/Bp stars ($1.5 M_{\odot}$ to $6 M_{\odot}$) host magnetic fields with mean strengths ranging from 200 G to 30 kG.

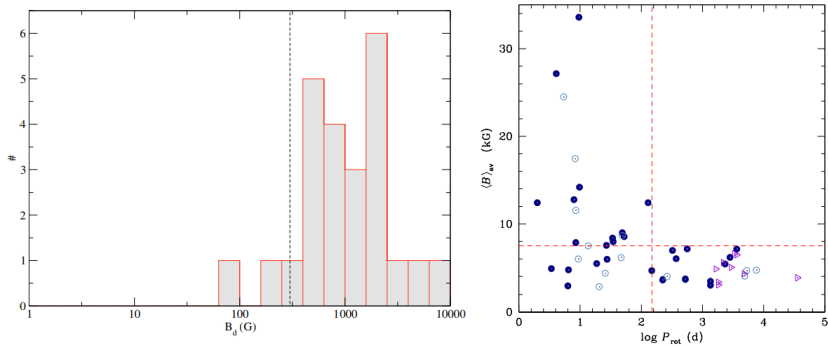


Figure: Left panel: Histogram of best fit dipole field strengths, from the sample of 27 Ap/Bp stars of [Aurière et al. \(2007\)](#). Right panel: Observed mean magnetic field modulus against rotation period ([Mathys, 2017](#)).

Possible explanations

The dynamo is driven by the convective core of the star
[\(Krause & Oetken, 1976\)](#).

Previous work

[Brun et al. \(2005\)](#) performed simulations of the inner 30% by radius (where 15% is the core) of a $2 M_{\odot}$ A-type star, obtaining magnetic fields with typical strengths around the equipartition value with kinetic energy. [Augustson et al. \(2016\)](#) modeled the core dynamo of a $10 M_{\odot}$ B-type star.

Possible explanations

Surface magnetic field?

In principle, magnetic structures created by the core dynamo could reach the surface due to buoyancy. However, this process has a timescale longer than the main-sequence life of the star ([Parker, 1979](#); [Moss, 1989](#)), unless very small structures are considered ([MacGregor & Cassinelli, 2003](#)).

Possible explanations (2)

Fossil field surviving from the star formation ([Cowling, 1945](#)).

Previous work

[Braithwaite & Nordlund \(2006\)](#) performed 3D simulations of a $2M_{\odot}$, $R = 1.8R_{\odot}$ A-type star, inside a box of side $l = 4.5R$ using a grid of 96^3 . They found stable axisymmetric magnetic field configurations in a radiative interior starting with random field initial conditions. Recently, similar results were found by [Becerra et al. \(2022\)](#).

Possible explanations (2)

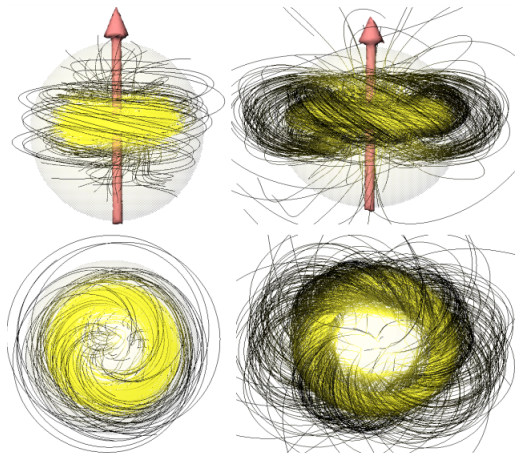


Figure: Stable magnetic field configurations from Braithwaite & Nordlund (2006). The upper plots correspond to snapshots with $t = 22.6$ days (left) and $t = 31.9$ days (right). The lower plots are the same snapshots displayed from a different angle.

Possible explanations (3)

Interaction between a core dynamo and a fossil field.

Previous work

Featherstone et al. (2009) performed 3D simulations of the inner 30% by radius of a $2M_{\odot}$ A-type star (excluding the innermost values), modeling a core dynamo surrounded by a radiative envelope. The inclusion of a fossil field in this envelope can lead to a very strong super-equipartition field.

Possible explanations (3)

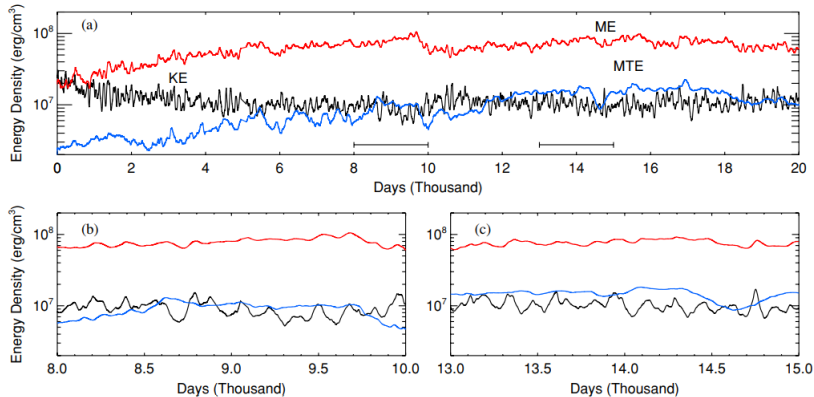


Figure: Temporal evolution of overall energy densities after imposing a mixed poloidal-toroidal magnetic (fossil) field configuration. The magnetic energy (ME) grows until it reaches 10 times the value of the kinetic energy (KE) ([Featherstone et al., 2009](#)).

Possible explanations (4)

Some additional theories:

- **Taylor-Spruit dynamo** ([Spruit, 2002](#)): it is a result of the interaction between a magnetic instability (e.g. [Taylor, 1973](#)) and differential rotation.
- **Subsurface convection** ([Cantiello et al., 2009](#)): stellar models predicts convection close to the surface due to bumps in the stellar opacities. These layers can host dynamos ([Cantiello & Braithwaite, 2019](#)).

The setup

To explore the core dynamo scenario, we model a star of radius R , inside a box of side $l = 2.2R$ ([Dobler et al., 2006; Käpylä, 2021](#)).

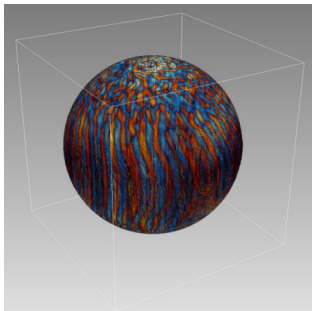


[Figure: Star-in-a-box model, image courtesy of Petri Käpylä.](#)

Stellar parameters:

$$R_* = 2.1R_\odot$$

$$M_* = 2.2M_\odot$$

$$L_* = 23.5L_\odot$$

$$\rho_0 = 5.5 \cdot 10^4 \text{ g/m}^3$$

$$g_{\text{surf}} = 137 \text{ m/s}^2$$

The simulations were run with the PENCIL CODE.

The model

We solve the fully compressible non-ideal MHD equations:

$$\frac{\partial \mathbf{A}}{\partial t} = \mathbf{U} \times \mathbf{B} - \eta \mu_0 \mathbf{J}, \quad (1)$$

$$\frac{D \ln \rho}{Dt} = -\nabla \cdot \mathbf{U}, \quad (2)$$

$$\frac{D \mathbf{U}}{Dt} = -\nabla \Phi - \frac{1}{\rho} (\nabla p - \nabla \cdot 2\nu \rho \mathbf{S} + \mathbf{J} \times \mathbf{B}) - 2\boldsymbol{\Omega} \times \mathbf{U} + \mathbf{f}_d, \quad (3)$$

$$T \frac{Ds}{Dt} = -\frac{1}{\rho} [\nabla \cdot (\mathbf{F}_{\text{rad}} + \mathbf{F}_{\text{SGS}}) + \mathcal{H} - \mathcal{C} + \mu_0 \eta \mathbf{J}^2] + 2\nu \mathbf{S}^2, \quad (4)$$

where $D/Dt = \partial/\partial t + \mathbf{U} \cdot \nabla$ is the advective derivative,
 $\mathbf{B} = \nabla \times \mathbf{A}$, the relation between \mathbf{J} and \mathbf{B} is given by the Ohm's law $\mathbf{J} = \nabla \times \mathbf{B}/\mu_0$.

The model (2)

The radiative and SGS entropy fuxes are

$$\mathbf{F}_{\text{rad}} = -K \nabla T, \quad \mathbf{F}_{\text{SGS}} = -\chi_{\text{SGS}} \rho \nabla s', \quad (5)$$

respectively, where K is the radiative heat conductivity, χ_{SGS} is the SGS diffusion coefficient, and $s' = s - \langle s \rangle_t$ is the fluctuating entropy.

The model (2)

The radiative and SGS entropy fuxes are

$$\mathbf{F}_{\text{rad}} = -K \nabla T, \quad \mathbf{F}_{\text{SGS}} = -\chi_{\text{SGS}} \rho \nabla s', \quad (5)$$

respectively, where K is the radiative heat conductivity, χ_{SGS} is the SGS diffusion coefficient, and $s' = s - \langle s \rangle_t$ is the fluctuating entropy.

The heating and cooling terms are

$$\mathcal{H}(r) = \frac{L_{\text{sim}}}{(2\pi w_L^2)^{3/2}} \exp\left(-\frac{r^2}{2w_L^2}\right), \quad \mathcal{C}(\mathbf{x}) = \rho c_P \frac{T(\mathbf{x}) - T_{\text{surf}}}{\tau_{\text{cool}}} f_e(r),$$

The model (3)

Following [Käpylä \(2022\)](#), we used radial profiles for the diffusivities ν and η , such that radiative layers have values 10^2 times smaller than the core.

We defined two groups:

Group MHD:

- $r_{\text{start}} = 0.35R$
- $w = 0.06R$

Group MHD*:

- $r_{\text{start}} = 0.3R$
- $w = 0.03R$

The model (3)

Following [Käpylä \(2022\)](#), we used radial profiles for the diffusivities ν and η , such that radiative layers have values 10^2 times smaller than the core.

We defined two groups:

Group MHD:

- $r_{\text{start}} = 0.35R$
- $w = 0.06R$

Group MHD*:

- $r_{\text{start}} = 0.3R$
- $w = 0.03R$

The problem: these values are hard to resolve using our current resolution.

The model (3)

Following [Käpylä \(2022\)](#), we used radial profiles for the diffusivities ν and η , such that radiative layers have values 10^2 times smaller than the core.

We defined two groups:

Group MHD:

- $r_{\text{start}} = 0.35R$
- $w = 0.06R$

Group MHD*:

- $r_{\text{start}} = 0.3R$
- $w = 0.03R$

The problem: these values are hard to resolve using our current resolution.

Solution: Hyperdiffusivity terms. Resolution-independent mesh hyper-Reynolds number method (see [Lyra et al., 2017](#)).

Initial conditions

The convective core is assumed to encompass 20% of the stellar radius (similar to [Brun et al. 2005](#)).

We assume a piecewise polytropic initial state: $p(\rho) = K_0 \rho^\gamma$, where $\gamma = 1 + \frac{1}{n}$, and:

$$n = \begin{cases} 1.5 & \text{if } r < 0.2R \\ 3.25 & \text{if } r > 0.2R \end{cases},$$

is the polytropic index.

The flow and magnetic field start with Gaussian noise with amplitudes of $U_0 = 2 \cdot 10^{-3}$ m/s and $B_0 = 1$ G respectively.

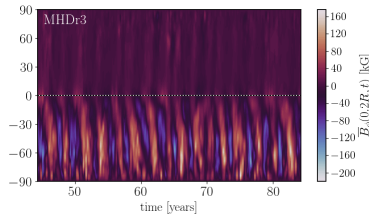
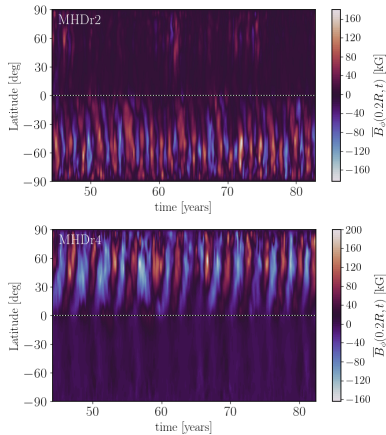
Simulations

Summary of the simulations:

Run	P_{rot} [days]	u_{rms} [m/s]	B_{rms} [kG]	Co	Ta[10^8]	Pe	Re	Re_M	$\text{Ri}_\Omega[10^{-2}]$
MHDr1	20	99	no dynamo	5.0	1.10	11	52	36	16.0
MHDr2	15	51	60	10.1	1.95	7	35	24	9.2
MHDr2*	15	52	57	9.9	1.95	7	35	25	9.2
MHDr3	10	39	65	19.2	4.38	5	27	19	4.1
MHDr3*	10	39	62	18.8	4.38	5	28	19	3.9
MHDr4	8	35	60	26.9	6.84	5	24	17	2.6
MHDr4*	8	35	57	26.2	6.84	5	25	17	2.5

$$P_{\text{rot}} = \frac{2\pi}{\Omega_0}, \quad \text{Co} = \frac{2\Omega_0}{u_{\text{rms}} k_R}, \quad \text{Ta} = \frac{4\Omega_0^2 \Delta r^4}{\nu^2}, \quad \text{Pe} = \frac{u_{\text{rms}}}{\chi_{\text{SGS}} k_R},$$
$$\text{Re} = \frac{u_{\text{rms}}}{\nu k_R}, \quad \text{Re}_M = \frac{u_{\text{rms}}}{\eta k_R}, \quad \text{Ri}_\Omega = \frac{N^2}{\Omega_0^2}.$$

Core dynamos



Run	\bar{B}_ϕ^{\min}	$\bar{B}_\phi^{\text{rms}}$	\bar{B}_ϕ^{\max}
MHD ^r 2	-182.1	31.6	178.0
MHD ^r 3	-216.9	35.2	175.7
MHD ^r 4	-162.0	35.8	197.9

Figure: Time-latitude diagrams of the azimuthally averaged toroidal magnetic field $\bar{B}_\phi(r = 0.2R, \theta, t)$ of the runs in the MHD group.

Core dynamos (2)

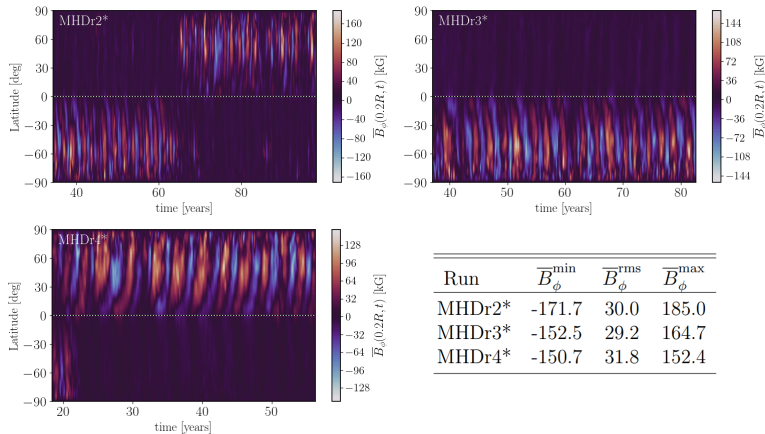


Figure: Time-latitude diagrams of the azimuthally averaged toroidal magnetic field $\bar{B}_\phi(r = 0.2R, \theta, t)$ of the runs in the MHD* group.

Comparison with other simulations

THE ASTROPHYSICAL JOURNAL LETTERS, 902:L3 (6pp), 2020 October 10

© 2020. The Author(s). Published by the American Astronomical Society.

OPEN ACCESS

<https://doi.org/10.3847/2041-8213/abb9a4>



Single-hemisphere Dynamos in M-dwarf Stars

Benjamin P. Brown¹ , Jeffrey S. Oishi² , Geoffrey M. Vasil³ , Daniel Lecoanet⁴ , and Keaton J. Burns^{5,6}

¹ Department Astrophysical and Planetary Sciences & LASP, University of Colorado, Boulder, CO 80309, USA; bpbrown@colorado.edu

² Department of Physics and Astronomy, Bates College, Lewiston, ME 04240, USA

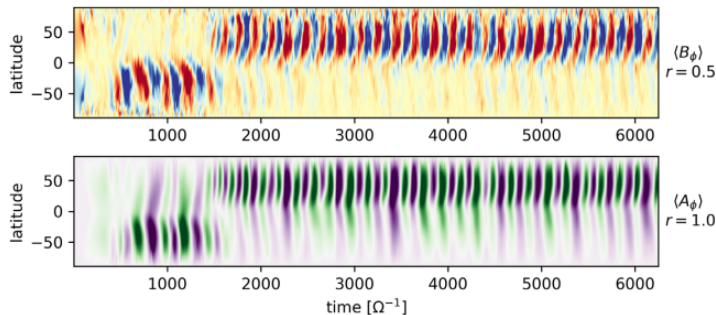
³ School of Mathematics and Statistics, University of Sydney, Sydney, NSW 2006, Australia

⁴ Department of Engineering Science and Applied Mathematics, Northwestern University, 2145 Sheridan Road, Evanston, IL 60208, USA

⁵ Department of Mathematics, Massachusetts Institute of Technology, Cambridge, MA 02139, USA

⁶ Center for Computational Astrophysics, Flatiron Institute, New York, NY 10010, USA

Received 2020 August 4; revised 2020 September 11; accepted 2020 September 17; published 2020 October 7



Comparison with other simulations (2)

A&A 678, A82 (2023)

<https://doi.org/10.1051/0004-6361/202244666>

© The Authors 2023

Astronomy
Astrophysics

Simulations of dynamo action in slowly rotating M dwarfs: Dependence on dimensionless parameters

C. A. Ortiz-Rodríguez¹, P. J. Käpylä^{2,3,4}, F. H. Navarrete^{5,4}, D. R. G. Schleicher¹, R. E. Mennickent¹,
J. P. Hidalgo¹, and B. Toro-Velásquez¹

¹ Departamento de Astronomía, Facultad de Ciencias Físicas y Matemáticas, Universidad de Concepción, Av. Esteban Iturra s/n
Barrio Universitario, Casilla 160-C, Chile

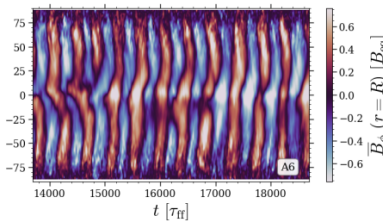
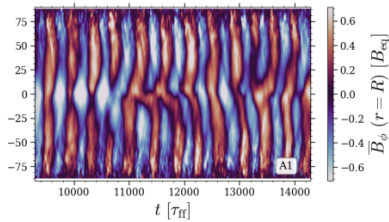
e-mail: ortizrodcarolina@gmail.com

² Leibniz-Institut für Sonnenphysik (KIS), Schöneckstr. 6, 79104 Freiburg, Germany

³ Institut für Astrophysik und Geophysik, Georg-August-Universität Göttingen, Friedrich-Hund-Platz 1, 37077 Göttingen, Germany

⁴ Nordita, KTH Royal Institute of Technology and Stockholm University, 10691 Stockholm, Sweden

⁵ Hamburger Sternwarte, Universität Hamburg, Gojenbergsweg 112, 21029 Hamburg, Germany



Comparison with observations

Monthly Notices
of the
ROYAL ASTRONOMICAL SOCIETY

MNRAS 512, L16–L20 (2022)
Advance Access publication 2022 February 11



<https://doi.org/10.1093/mnrasl/slac013>

Asteroseismic inference of the near-core magnetic field strength in the main-sequence B star HD 43317

Daniel Lecoanet ^{①,2,3}★ Dominic M. Bowman^{3,4} and Timothy Van Reeth^{3,4}

¹Department of Engineering Sciences and Applied Mathematics, Northwestern University, Evanston, IL 60208, USA

²CIERA, Northwestern University, Evanston, IL 60201, USA

³Kavli Institute for Theoretical Physics, University of California, Santa Barbara, CA 93106, USA

⁴Institute of Astronomy, KU Leuven, Celestijnenlaan 200D, B-3001 Leuven, Belgium

Accepted 2022 February 3. Received 2022 February 3; in original form 2021 December 22

ABSTRACT

About 10 per cent of intermediate- and high-mass dwarf stars are observed to host a strong large-scale magnetic field at their surface, which is thought to be of fossil field origin. However, there are few inferences as to the magnetic field strength and geometry within the deep interiors of stars. Considering that massive stars harbour a convective core whilst on the main sequence, asteroseismology of gravity (g) modes is able to provide constraints on their core masses, yet it has so far not been used to probe the strength of their interior magnetic fields. Here, we use asteroseismology to constrain an upper limit for the magnetic field strength in the near-core region of the pulsating and magnetic B star HD 43317, based on the expected interaction of a magnetic field and its g modes. We find a magnetic field strength of order 5×10^5 G is sufficient to suppress high-radial order g modes and reproduce the observed frequency spectrum of HD 43317, which contains only high-frequency g modes. This result is the first inference of the magnetic field strength inside a main-sequence star.

Key words: asteroseismology – stars: individual: HD 43317 – stars: magnetic field – stars: oscillations.

Surface magnetic fields

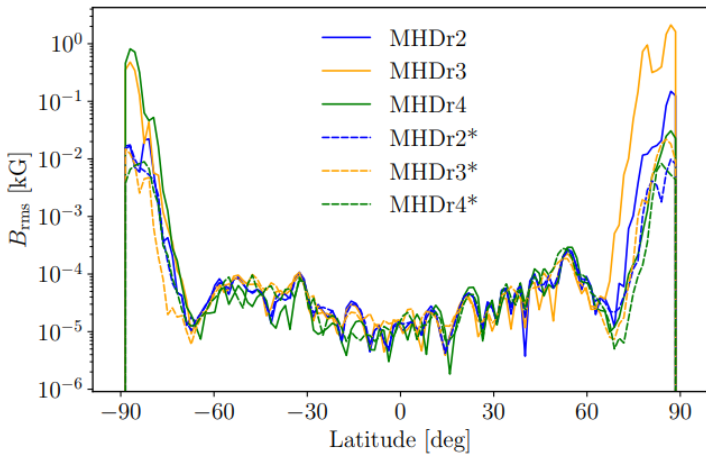
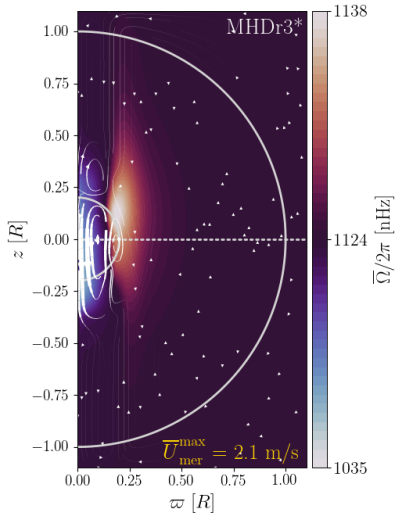


Figure: Time averaged root-mean-square magnetic field as a function of latitude of runs from groups MHD and MHD*.

Large-scale flows



The averaged rotation rate is given by:

$$\bar{\Omega}(\varpi, z) = \Omega_0 + \bar{U}_\phi(\varpi, z)/\varpi.$$

The averaged meridional flow is defined as:

$$\bar{\mathbf{U}}_{mer}(\varpi, z) = (\bar{U}_\varpi, 0, \bar{U}_z).$$

Figure: Profile of $\bar{\Omega}(\varpi, z)$ for MHD³.

Large-scale flows (2)

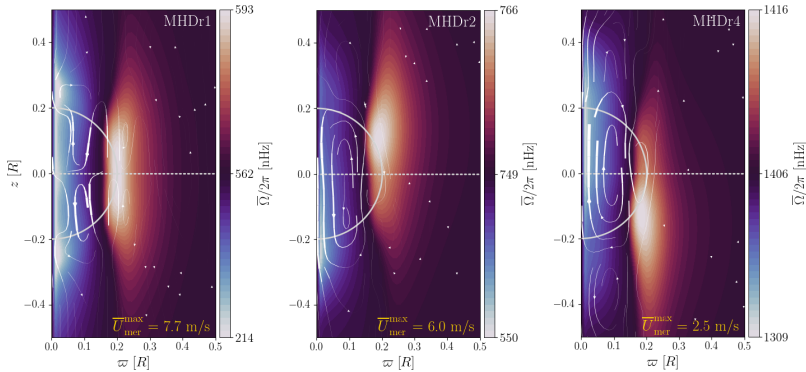


Figure: Profiles of the temporally and azimuthally averaged rotation rate $\bar{\Omega}(\varpi, z)$ for runs in the MHD group. The streamlines indicate the mass flux due to meridional circulation and the maximum averaged meridional flow is indicated in the lower right side of each plot.

Large-scale flows (3)

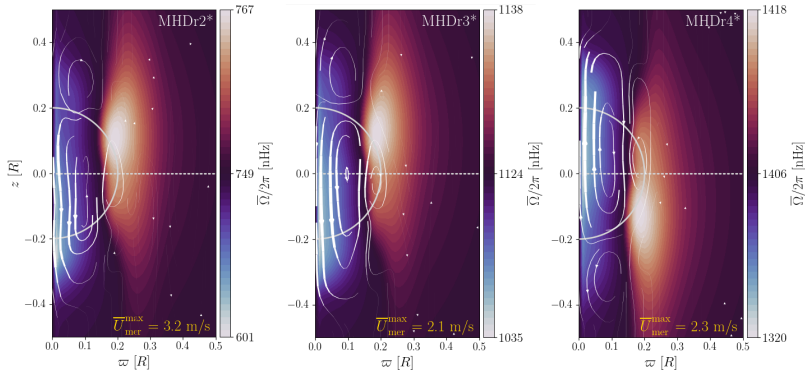


Figure: Profiles of the temporally and azimuthally averaged rotation rate $\bar{\Omega}(\varpi, z)$ for runs in the MHD* group. The streamlines indicate the mass flux due to meridional circulation and the maximum averaged meridional flow is indicated in the lower right side of each plot.

Comparison with observations

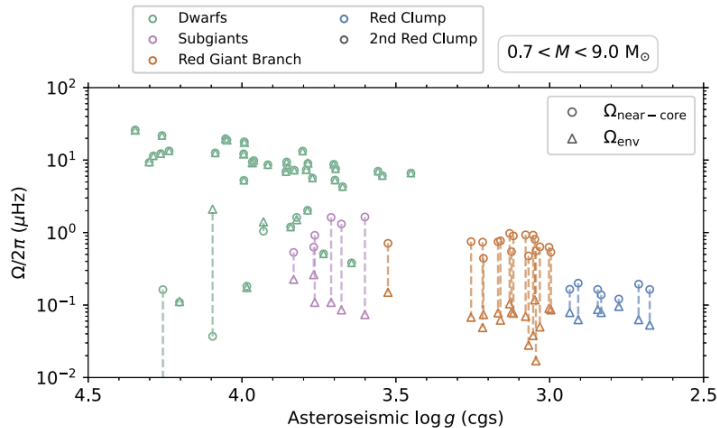
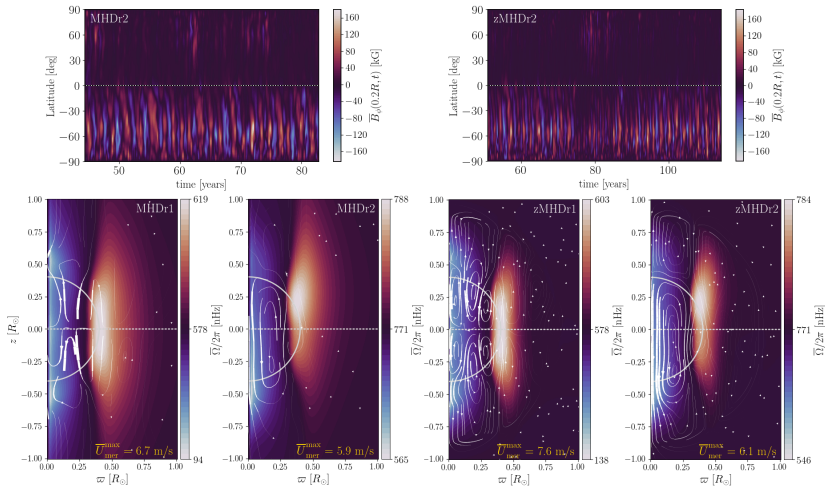


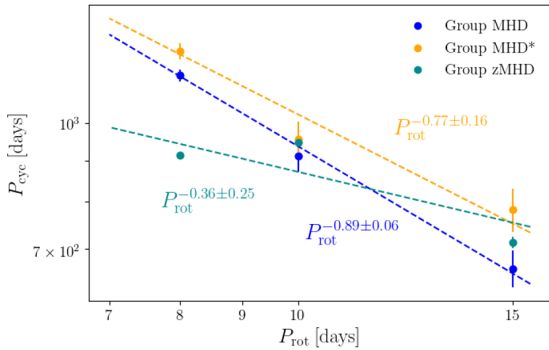
Figure: Sample of stars at different evolutionary stages with an asteroseismic estimate of rotation as a function of asteroseismic $\log g$. Adapted from [Bowman \(2023\)](#).

Zoom setup

The zMHD group is essentially the same as the main-sequence model, but $l = 1.1R$.
Excluding half of the star, yields higher resolution in the core.



Rotational scaling of magnetic cycles



Run	P_{rot} [days]	P_{cyc} [years]
MHDr1	20	-
MHDr2	15	1.81 ± 0.10
MHDr2*	15	2.14 ± 0.13
MHDr3	10	2.50 ± 0.11
MHDr3*	10	2.62 ± 0.14
MHDr4	8	3.14 ± 0.05
MHDr4*	8	3.37 ± 0.08

Figure: The magnetic cycle period P_{cyc} as a function of the rotation period P_{rot} .

Rotational scaling of magnetic cycles (2)

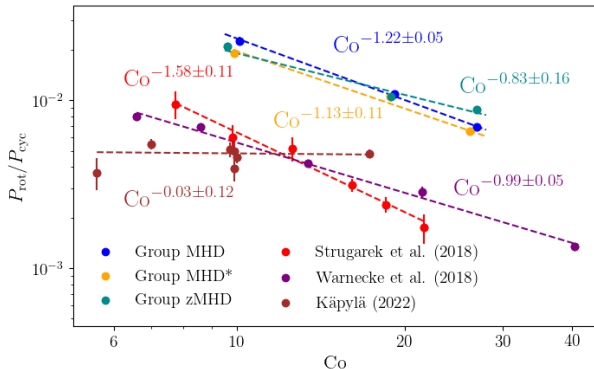


Figure: Ratios of rotation to cycle period as a function of the Coriolis number. Additional data are from Strugarek et al. (2018, red), Warnecke (2018, purple) and Käpylä (2022, brown). The dashed lines are the best power-law fits to the data.

Conclusions

Conclusions

- The core of the star is able to produce strong magnetic fields ($B_{\text{rms}} \approx 60$ kG, $\overline{B}_{\phi}^{\max} \approx 200$ kG).
- A core dynamo does not seem to be sufficient to explain the large-scale surface magnetic fields of Ap stars.
- A substantial part of the radiative envelope has approximately-rigid rotation. The core has solar-like differential rotation in all runs.
- In the core dynamo, there is an inverse relation between P_{rot} and P_{cyc} .

Future work

- The wide range of observed magnetic field strengths, and their often simple geometries seem to indicate fossil fields.

Future work

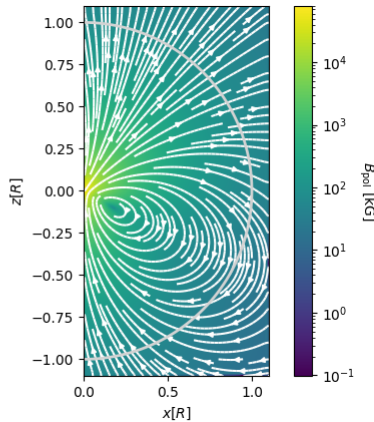
- The wide range of observed magnetic field strengths, and their often simple geometries seem to indicate fossil fields.
- However, as the core dynamo produces dynamically relevant magnetic fields it should not be neglected when fossil fields are explored (e.g. [Featherstone et al., 2009](#); [Lecoanet et al., 2022](#)).

Future Work (2)

- Explore how the core dynamo changes in the presence of a fossil field.

$$\mathbf{m}(\theta) = A_0 \sin \theta \hat{x} + A_0 \cos \theta \hat{z},$$

$$\begin{aligned} \mathbf{A}(r, \theta) = & -\frac{A_0 y \cos \theta}{r^3} \hat{x} \\ & + A_0 \left(\frac{x \cos \theta - z \sin \theta}{r^3} \right) \hat{y} \\ & + \frac{A_0 y \sin \theta}{r^3} \hat{z}. \end{aligned}$$



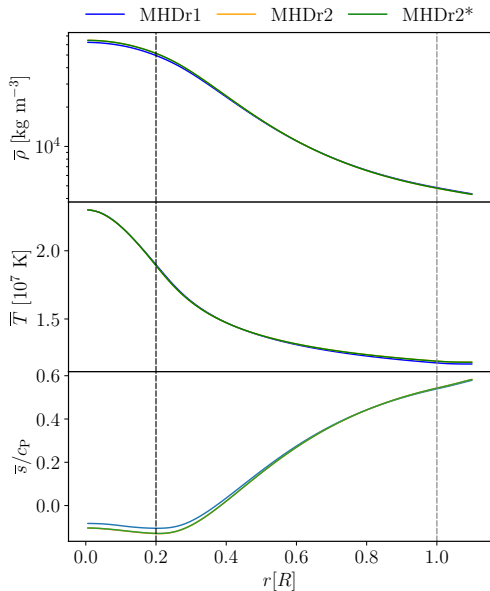
References I

- Augustson K. C., Brun A. S., Toomre J., 2016, *ApJ*, 829, 92
- Aurière M., et al., 2007, *A&A*, 475, 1053
- Becerra L., Reisenegger A., Valdivia J. A., Gusakov M. E., 2022, *MNRAS*, 511, 732
- Bowman D. M., 2023, *Ap&SS*, 368, 107
- Braithwaite J., Nordlund Å., 2006, *A&A*, 450, 1077
- Brandenburg A., Subramanian K., 2005, *Phys. Rep.*, 417, 1
- Brun A. S., Browning M. K., Toomre J., 2005, *ApJ*, 629, 461
- Cantiello M., Braithwaite J., 2019, *ApJ*, 883, 106
- Cantiello M., et al., 2009, *A&A*, 499, 279
- Cowling T. G., 1945, *MNRAS*, 105, 166
- Dobler W., Stix M., Brandenburg A., 2006, *ApJ*, 638, 336
- Featherstone N. A., Browning M. K., Brun A. S., Toomre J., 2009, *ApJ*, 705, 1000
- Käpylä P. J., 2021, *A&A*, 651, A66
- Käpylä P. J., 2022, *ApJ*, 931, L17
- Krause F., Oetken L., 1976, in Weiss W. W., Jenkner H., Wood H. J., eds, IAU Colloq. 32: Physics of Ap Stars. p. 29
- Lecoanet D., Bowman D. M., Van Reeth T., 2022, *MNRAS*, 512, L16
- Lyra W., McNally C. P., Heinemann T., Masset F., 2017, *AJ*, 154, 146

References II

- MacGregor K. B., Cassinelli J. P., 2003, *ApJ*, 586, 480
- Mathys G., 2017, *A&A*, 601, A14
- Moss D., 1989, *MNRAS*, 236, 629
- Parker E. N., 1979, *Ap&SS*, 62, 135
- Spruit H. C., 2002, *A&A*, 381, 923
- Strugarek A., Beaudoin P., Charbonneau P., Brun A. S., 2018, *ApJ*, 863, 35
- Taylor R. J., 1973, *MNRAS*, 161, 365
- Warnecke J., 2018, *A&A*, 616, A72

Radial profiles



Meridional distribution

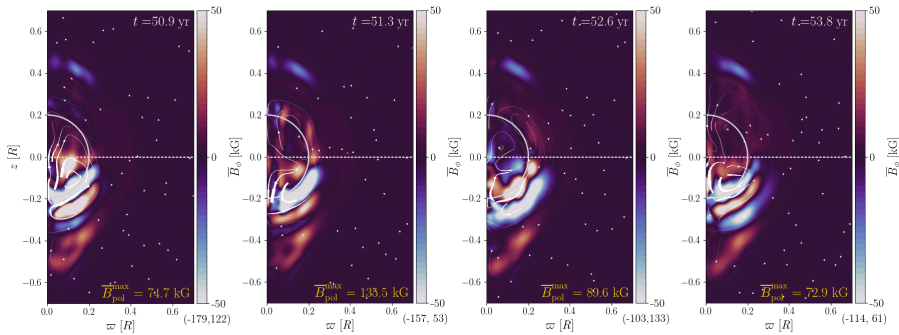


Figure: Azimuthally averaged toroidal magnetic field from 1 cycle (~ 3 yrs).

Meridional distribution

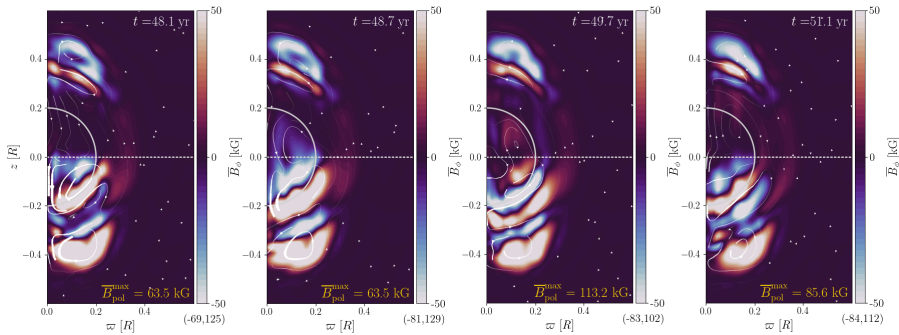


Figure: Azimuthally averaged toroidal magnetic field from 1 cycle (~ 3 yrs).